USING COMPUTER SIMULATIONS TO HELP UNDERSTAND FLOW STATISTICS AND STRUCTURES AT THE AIR-OCEAN INTERFACE

BY LIAN SHEN AND DICK K.P. YUE

The interaction among atmosphere, oceans, and surface waves is an important process with many oceanographic and environmental applications. It directly affects the motion and fate of pollutants such as oil spills. The oceans have an enormous capacity for mass and heat storage. The air-sea exchange of heat, humidity, momentum, and greenhouse gases directly affects short-term weather evolutions and long-term climate changes. In addition, the accurate prediction of air-sea interaction is of vital importance to many of the Navy's applications, including the operation of naval surface ships and remote sensing.

From the viewpoint of basic science, air-sea interaction is a challenging fluid-mechanics problem involving turbulence, waves, multiphase flows, and mixing, all of which operate at multiple temporal and spatial scales. The controlling transfer processes are the wind, ocean surface current, wave, and wave-breaking, all of which involve atmospheric and ocean flows in the vicinity of an air-water interface. Considerable work has been done to understand aspects of this problem in terms of simplified theory. Nevertheless, due to the complex nature of the physical problem, our current understanding of the mechanisms for the transport of mass, momentum, and heat within the atmosphere-ocean wave boundary layer is quite limited. In particular, the essential dynamics of the coupled air-sea boundary layers at small scales (say, from millimeters to tens of meters) remain elusive. As a result, existing theories and predic-tion tools have to rely on empirical parameterization. There is a critical need for a detailed study of the small-scale physics at the air-water interface, which is a foundation for the development of large-scale simulation and prediction tools.

In recent years, we have been using high-performance computers with powerful simulation capabilities as a research tool to investigate the mechanisms of air-sea interactions at small scales. In direct simulations, the governing equations for the coupled flow are solved numerically, typically with a fine computational grid. Even with very large computers, many of the underlying physical processes, generally associated with the turbulent nature of the flow, are not resolved. To allow the problem to be solved, or "closed," the numerical simulations require "closure models," which in effect express the unknown and non-resolved quantities in terms of those that are known or resolved in the simulation. Such closure models aim to capture the underlying physical mechanisms and are typically expressed in terms of variables or parameters describing the overall problem. These parameterizations are usually guided by finer-resolution direct simulations that do not contain the closure models. The purpose of our numerical study is to complement field and laboratory measurement and theoretical investigation. With collaboration among different disciplines, we hope to obtain improved physical understanding and parameterization of air-sea interactions.

$$\underline{\Omega} = (\partial u_i/\partial x_j - \partial u_j/\partial x_i)$$

$$\frac{\underline{S}^2 + \underline{\Omega}^2}{}$$

$$\partial u/\partial x + \partial v/\partial y$$

Air

Water

...we have been using high-performance computers with powerful simulation capabilities as a research tool to investigate the mechanisms of air-sea interactions at small scales.

In our study, the basic equations governing the conservation of mass and momentum of the air and water turbulent flows, namely the continuity equation and the Navier-Stokes equations, are solved numerically. An inherent challenge in turbulence simulation is the requirement to capture the effects of all the flow structures, often referred

To augment DNS and to extend the results to larger-scale problems, we use a second approach called large-eddy simulation (LES). In LES, only the large eddies are simulated directly while the effects of small eddies (smaller than the numerical grid scales) are modeled. With high-performance computing using $O(10^7)$ grid points, LES allows us

physical properties of air and water, and the complexity associated with free-surface motions, especially with waves. The density of water is three orders of magnitude larger than that of air, and the water kinematic viscosity is one order of magnitude smaller than that for air[1]. Because of such disparity, the interaction between air and water possesses many unique features not seen in other two-phase fluid flows. In our simulations, the air and water motions interact with each other through the kinematic and dynamic free-surface boundary conditions at the air-water interface. The former states that a fluid particle at the interface stays on the interface, while the latter specifies the balance of forces across the air-water interface. These two boundary conditions are coupled though a novel alternating scheme. Details of our numerical method can be found in Liu (2005). The effects of surface waves for these flows are captured in the simulations. Depending on the sea state (or wave steepness), a number of treatments are developed: (1) at low wind speeds when the surface is almost flat, a fixed-grid approach with the option of linearized boundary conditions for free-surface deformations, (2) at moderate wind speeds, a bound-

> There is a critical need for a detailed study of the small-scale physics at the air-water interface, which is a foundation for the development of large-scale simulation and prediction tools.

to as "turbulent eddies," of which the size spans a wide range of scales. In our study, we employ two approaches. The first is direct numerical simulation (DNS), which resolves all eddies explicitly. The demand on computing resources is high and in most cases we are limited to simple, idealized cases at small scales. Using state-of-the-art computations, typical physical problems that can be studied using DNS are limited to wind speeds of one to two meters per second over a small wavefield of the order of one meter. The DNS are useful for characterizing the underlying basic statistics, structures, and mechanisms, thus providing a useful quantitative picture of the overall dynamics. DNS has been shown to be a powerful research tool to elucidate detailed physical mechanisms in many other turbulent flows (e.g., the review by Moin and Mahesh, 1998).

to study problems with wind speeds of up to about 10 m/s blowing over a wave group. Spatially, this simulation could obtain resolutions of less than one meter horizontally and a few centimeters vertically. This simulation resolves the dynamically important flow structures, while the effects from sub-grid scales are included using closure models (effective ones typically are dissipation models of the Smagorinsky type). With this approach, the observations obtained using DNS and LES are consistent, elucidating the salient features of the air-water interactions. Because the DNS results show more of the finer-scale details, we focus below on the discussion based on our DNS simulations.

In addition to the multi-scale nature of turbulence, other great challenges in simulating air-sea coupled turbulent flows include the large difference in the

Lian Shen (lshen@mit.edu) is Assistant Professor, Department of Civil Engineering, Johns Hopkins University, Baltimore, MD, USA. **Dick K.P. Yue** is Associate Dean of Engineering and Professor of Hydrodynamics and Ocean Engineering, Department of Mechanical Engineering, Massachusetts Institute of Technology, Cambridge, MA, USA.

---

[1] The kinematic viscosity (=dynamic viscosity/density) of water is smaller than for air (by a factor of 10) because the density of water is about one thousand times greater than for air. From a fluid mechanics point of view, a fluid's kinematic viscosity is often the better way to view things. Heuristically, if dynamic viscosity is associated with the actual stress, then in terms of understanding the kinematics (e.g., velocity changes), what matters is not the magnitude of the stress, but the magnitude of the stress relative to the density of the fluid.

ary-interface-tracking method that directly captures wave-turbulence interactions with high accuracy, and (3) at high wind speeds as the waves steepen and break, an Eulerian-interface-capturing method based on the level set approach for the air-water mixed flow. A typical result using approach 2 is shown in Figure 1a. For moderate to high wave amplitude and steepness, the wave effects play an essential role in the air-sea interaction and must be accounted for. On the other hand, for small wave magnitudes typical under low-wind conditions, our extensive study shows that the presence of waves has a relatively minor effect on the overall flow dynamics (see, for example, Shen et al., 1999), while the surface roughness itself can be obtained from the underlying pressure field. In this article, we focus on relatively low wind speed when the waves are small. Accordingly, the results below are obtained using approach 1. The situation involving higher wind speeds and
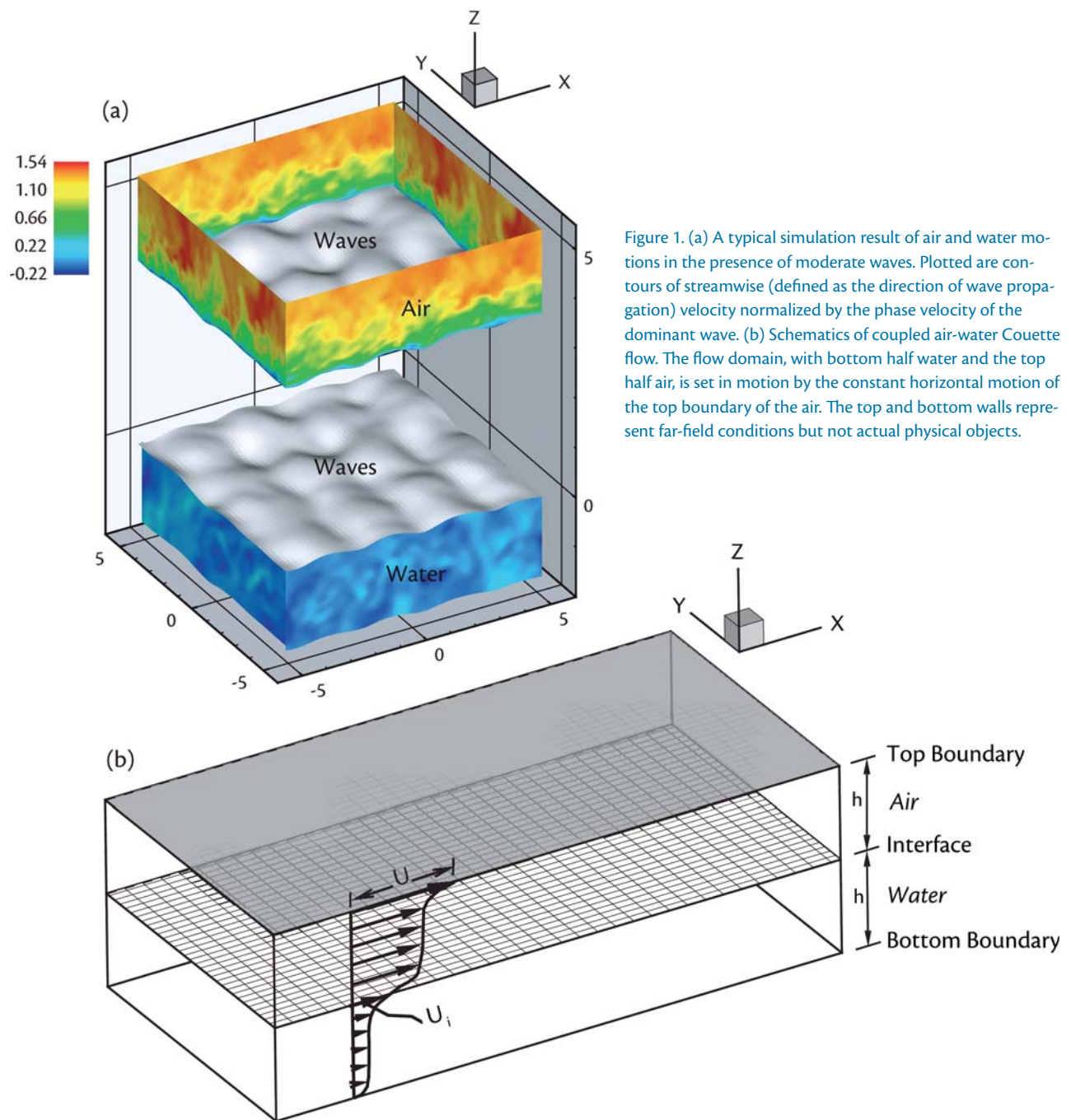

Figure 1. (a) A typical simulation result of air and water motions in the presence of moderate waves. Plotted are contours of streamwise (defined as the direction of wave propagation) velocity normalized by the phase velocity of the dominant wave. (b) Schematics of coupled air-water Couette flow. The flow domain, with bottom half water and the top half air, is set in motion by the constant horizontal motion of the top boundary of the air. The top and bottom walls represent far-field conditions but not actual physical objects.

large-amplitude waves is discussed in the last section.

Using systematic simulations on high-performance parallel computers with finely resolved temporal and spatial detail, we obtain a complete physical description of the turbulent air-sea flow field that fully captures air-water dynamics. This description provides a basis for the identification of key transport processes within the atmosphere-ocean boundary layer. Our objectives are to assess the key processes at the air-sea interface and to establish a physical foundation for the characterization and parameterization of the mass, momentum, and energy transfer between the atmosphere and oceans at small scales.

STATISTICS OF ATMOSPHERIC AND OCEAN FLOWS— A FIRST LOOK

As an example problem that contains all the key features of low-speed air-sea couple flow, we study the turbulent air-water Couette flow shown in Figure 1b. A controlling parameter for this problem is the Reynolds number based on the shear velocity at the interface, domain half-height, and kinematic viscosity of the fluids. For the case shown, this Reynolds number is 120 for the waterside motion and 270 for the airside motion. By examining the detailed flow characteristics at the air-water interface located in the middle of the domain, we obtain useful insights into the physics of interfacial

interactions representative of the coupled air-sea turbulent boundary layers. Of particular interest is to compare and contrast the physics and features near the air-water interface to those in classical boundary layers over a fixed solid wall, a subject that has been studied extensively for over a century.

The mean velocity profiles for the air and water turbulent motions for a representative case are plotted in Figure 2. Here and hereafter, unless otherwise pointed out, all the quantities are normalized by domain half-height and the air velocity at the top boundary. The stress balance across the air-water interface requires the product of dynamic viscosity and velocity gradient to be the
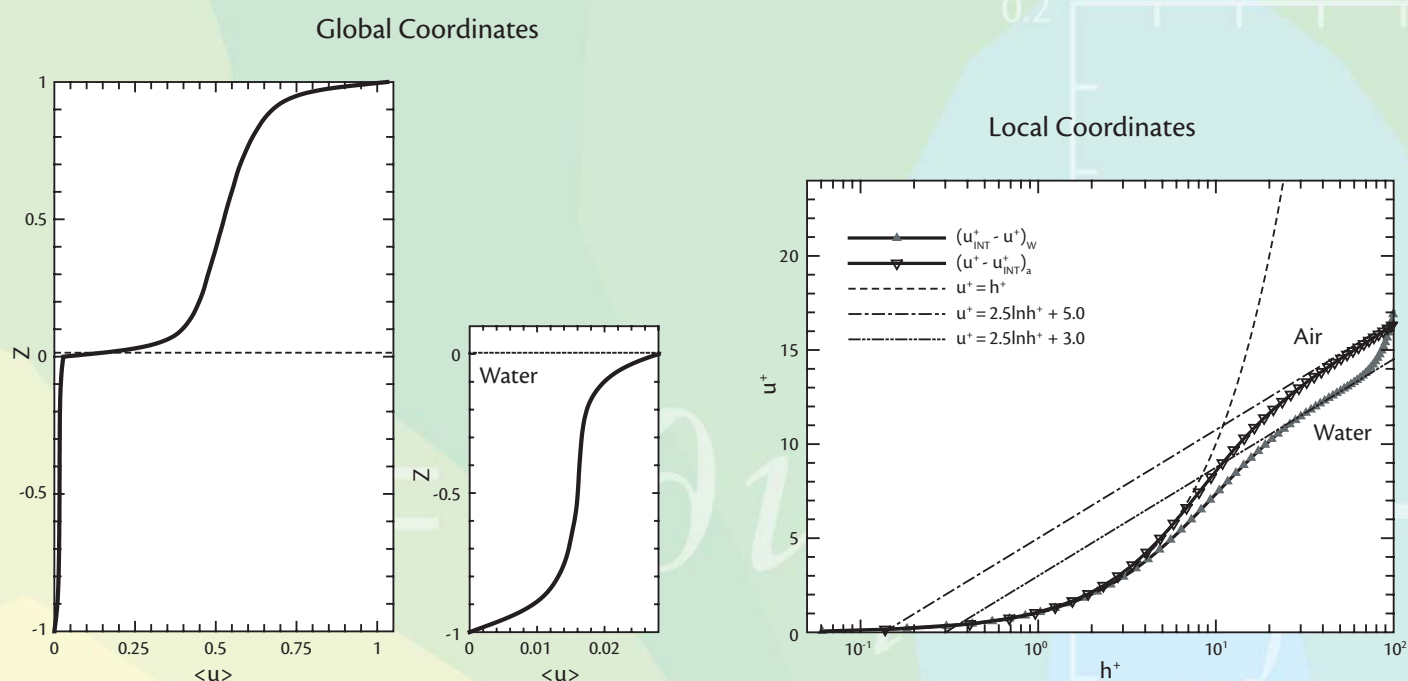

Figure 2. Left and middle: Air and water mean velocity profiles in global coordinates. Right: Variation of mean velocity near the air-water interface in local coordinates. In global coordinates, the quantities are normalized by domain half-height and the air velocity at the top boundary. In local coordinates, the velocity is normalized by friction velocity at the interface, and the distance from the interface is expressed in terms of a wall unit. Shown are the shear flow in the air and water and the comparison with the boundary layer theory. Triangles and squares are the results obtained from our study. The dashed curves are predictions by the linear law and the log law.

same at the two sides of the interface. Because the value of dynamic viscosity in water is significantly (63.7 times at 1 atm and 20°C) larger than that in air, the velocity gradient in the water is much smaller than that in the air. This is consistent with our experience that the wind speed is much larger than the water current velocity in the ocean. The middle figure in Figure 2 shows an enlarged velocity profile in water. It appears that the velocity variation near the air-water interface is similar to that near the solid (top and bottom) wall boundaries. To further investigate the near-interface behavior, the right figure in Figure 2 compares the velocity profiles in local coordinates. That is, all the physical quantities

are expressed by "wall units" based on the shear stress at the interface and fluid density, so that universal physical laws can be studied. It is seen that, very close to the interface, the mean velocities of both air and water are linear functions of the distances from the interface, while some distance away the velocities and distances satisfy a logarithmic law. This is the same as what we know happens in wall boundary layers. This resemblance is much more so on the airside (i.e., to the first order, the air-water interface behaves like a solid wall to air motions).

For the waterside, however, close examination shows that the viscous sublayer is thinner than that on the airside. The surface-layer structure can be seen

from the velocity profile in local coordinates. As shown in Figure 2, a linear law is valid close to the interface and a log law is valid away from the interface. In the semi-logarithm plot, the log law is represented by a straight line, which intersects with the velocity axis. This intersection point is lower in the water case than that in the air case (5.0 verses 3.0), which indicates that viscous sublayer region is smaller on the waterside. What causes the reduction in sublayer thickness in water? This, as it turns out, can be explained by the different restriction mechanisms of the interface on turbulence fluctuations. As shown in Figure 3, on the airside all the three velocity components diminish at the inter-
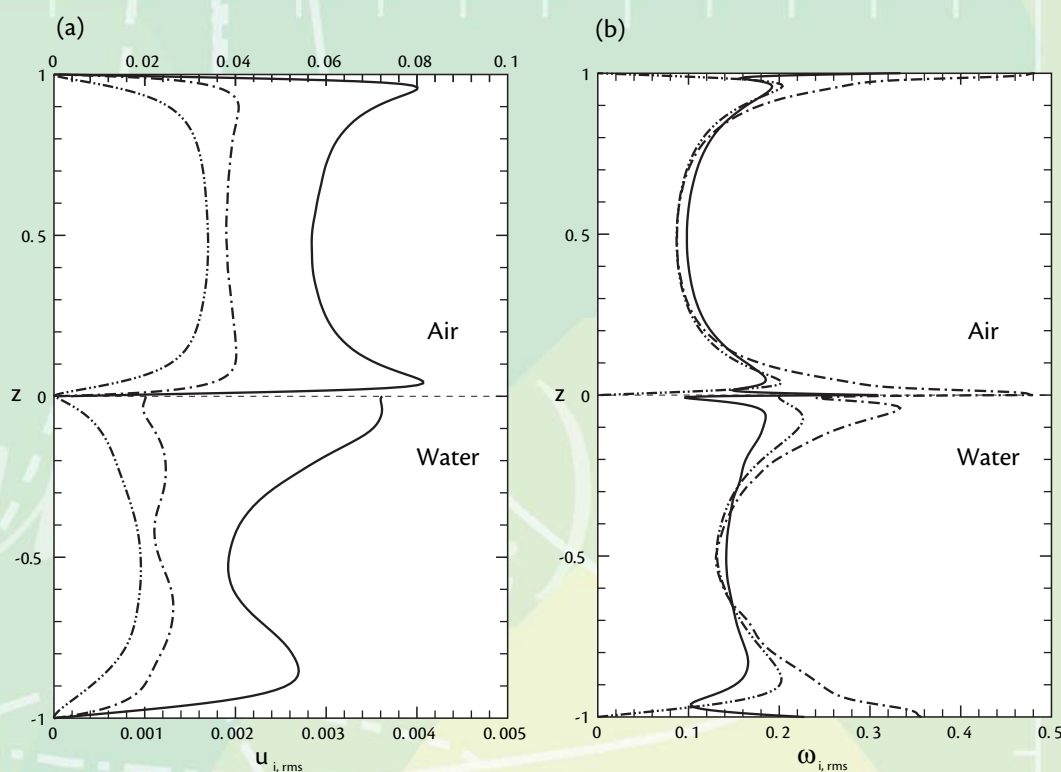

Figure 3. Profiles of (a) velocity and (b) vorticity fluctuations in the air and water. The solid lines are for the streamwise (x) components, the dash-dotted lines for the transverse (y) components, and the dash-dot-dotted lines for the vertical (z) components. A substantial difference exists at the interface ($z = 0$) between the air and water sides. The airside variation at the interface is similar to that at a solid wall, which is present at the top boundary ($z = 1$), while the waterside variation at the interface possesses features significantly different from those near the solid wall located at $z = -1$.

face. This is because the density of air is much less than that of water, and the air barely moves the water at the interface with the shear stress, so the interface acts more like a solid wall to the air motion. On the waterside, however, only the vertical velocity is reduced towards the interface. The water at the interface has much more freedom for horizontal motion relative to the case of a solid wall. Consequently, on the waterside, the viscous sublayer—where the turbulence transport is dominated by viscous diffusion—is much thinner in this case.

COHERENT VORTICAL STRUCTURES NEAR THE AIR-SEA INTERFACE

Vorticity is a measure of the angular motion of the flow. Coherent vortical structures are found to play an important role in turbulence transport processes (Robinson, 1991). A great advantage of simulation-based study is that it can provide whole-field (spatial and temporal) data for all the physical quantities computed. In this case, the computed three-dimensional vortical structures and their evolution can be identified. Figure 4a illustrates the typical vortical structures obtained from our simulation. The vorticity field in turbulence is usually complicated, and various techniques have been developed for an efficient representation of vortical structures. In our study, we employ the method developed by Jeong and Hussain (1995), in which the vortices are represented by the iso-surface of the second largest eigenvalue of the tensor $\underline{S}^2 + \underline{\Omega}^2$, with $\underline{S} = (\partial u_i/\partial x_j + \partial u_j/\partial x_i)$ and $\underline{\Omega} = (\partial u_i/\partial x_j - \partial u_j/\partial x_i)$ are respectively the symmetric and anti-symmetric parts

of the velocity gradient. This iso-surface has a strong correlation with the pressure minimum existing at the vortex core in high Reynolds flows, and it has been found to give a clear vortical indication for various types of turbulent flows. With this vortex definition, we find that vortical structures in the water near the interface can be characterized into mainly three categories: hairpin vortices, quasi-streamwise vortices, and interface-attached vortices. Representative vortices of these three types are illustrated in Figure 4a.

USE OF ADVANCED STATISTICAL TOOLS TO QUANTIFY FLOW STRUCTURES

As shown in Figure 4a, the instantaneous vortices in the turbulence field are rather complicated. Due to the chaotic nature of turbulence, a *specific* flow structure is generally not repeated in time or space. Furthermore, because of the fluctuations in the flow, a flow structure does not appear in a smooth, well-defined form. Rather, coherent structures emerge sharing key common features of the specific type of the structure in question, together with (smaller) distortions caused by turbulence noise. Although results like Figure 4a give us a qualitative description, for quantified results, other research tools are called for.

To quantify the effects of vortical structures, we employ a variable-interval space-averaging (VISA) technique (Kim, 1983), which is from the variable-interval time-averaging (VITA) method for laboratory experiments (Blackwelder and Kaplan, 1976). The VISA method, together with some other methods such as the stochastic estimation approach (Adrian

and Moin, 1988), has been found to be effective for turbulence-structure statistics. It is essentially a conditional averaging technique. For a specific flow structure, based on the instantaneous, three-dimensional flow field obtained from the simulations, we first use its key characteristics to identify the events when such structure appears. For each event, we isolate the flow field surrounding the structure being studied and then perform statistical averaging of these events. After a large number of ensemble averaging, we obtain converged statistics. Our experience shows that $O(10^3)$ events are usually needed. The details for the implementation of the VISA method are given in Shen and Yue (2001).

For the VISA statistics of air-sea turbulent coupled flows, the key to its success is the proper characterization of each flow structure so that when such structures appear in the flow field, they can be captured exclusively. For the three vortical structures shown in Figure 4a, we use, respectively, large streamwise vorticity component, ω_x, to characterize quasi-streamwise vortices; large positive transverse vorticity, ω_y, which corresponds to their head portion, to capture hairpin vortices; and large vertical vorticity, ω_z, which indicates the appearance of interface-connected vortices, to identify interface-attached vortices. We also use large magnitudes of the surface divergence, $\partial u/\partial x + \partial v/\partial y$, to identify upwellings and downwellings near the air-sea interface.

Figure 4b shows an example of the conditionally averaged results for hairpin vortex structures. Compared to the instantaneous vortex shown in Figure 4a, it is clear that the VISA method faithfully

(a)

Air

Interface

Scalar
Concentration

Water

Hairpin Vortex

Interface-attached Vortex

Quasi-streamwise Vortex
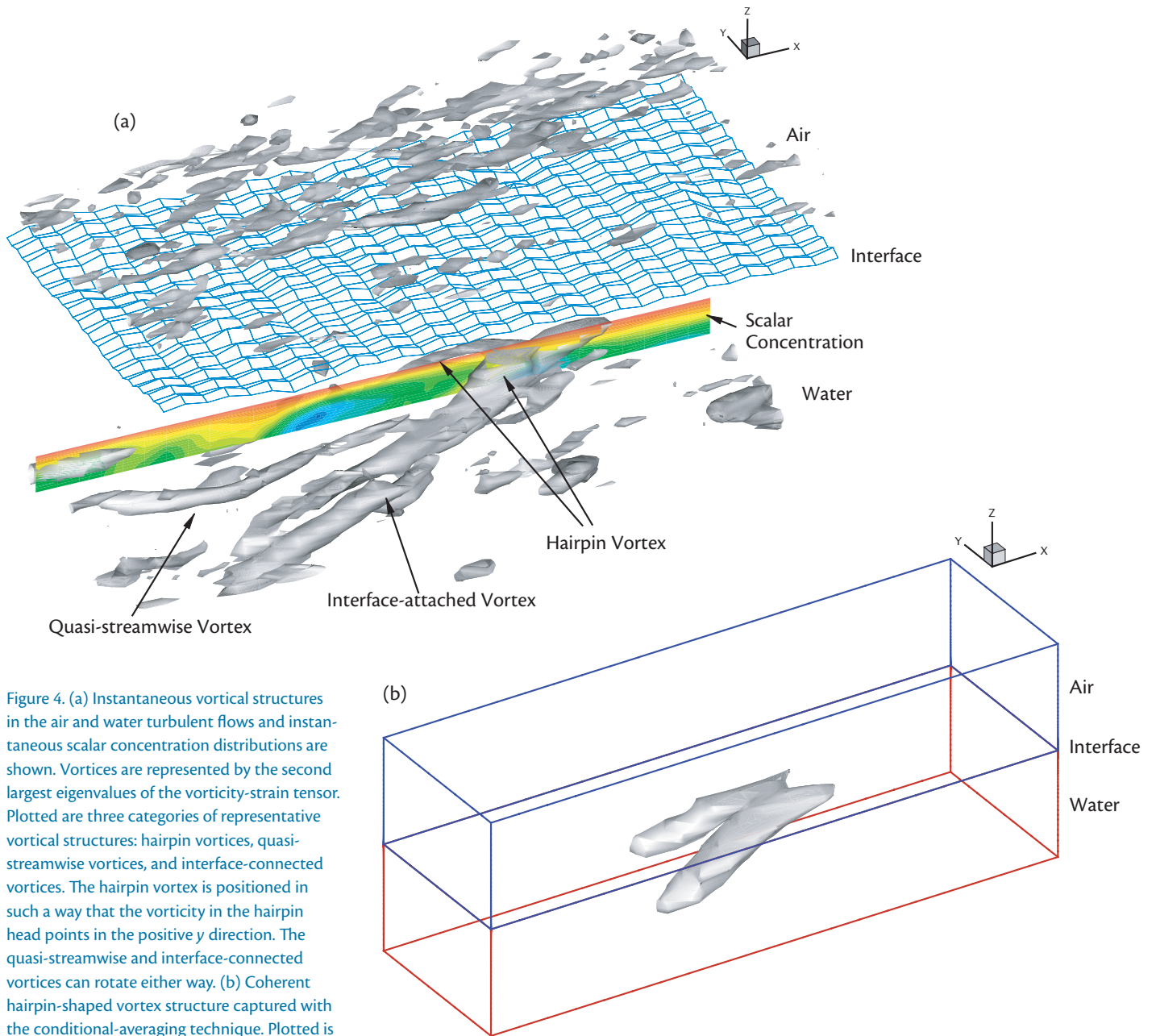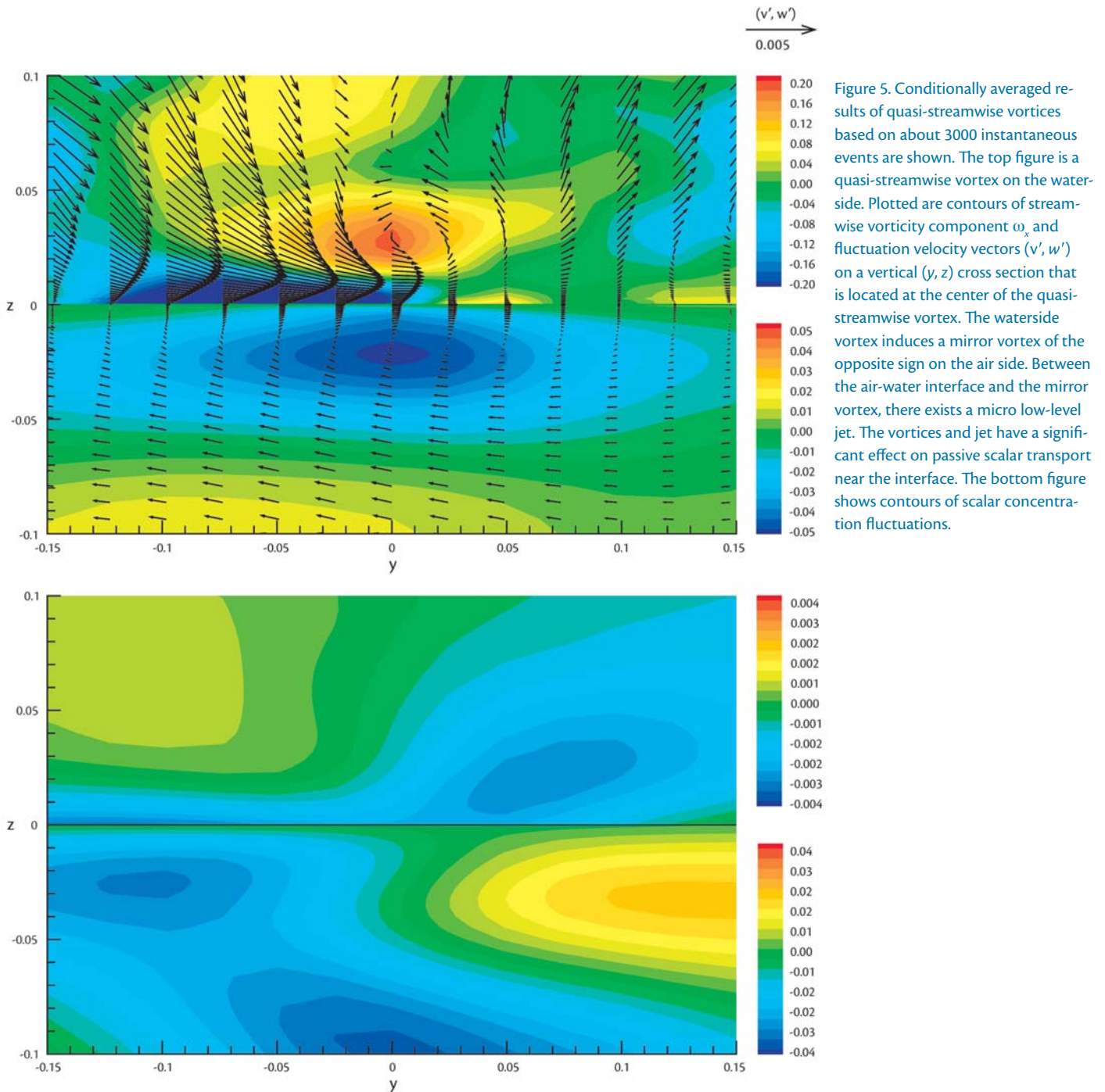
(b)

Air

Interface

Water

Figure 4. (a) Instantaneous vortical structures in the air and water turbulent flows and instantaneous scalar concentration distributions are shown. Vortices are represented by the second largest eigenvalues of the vorticity-strain tensor. Plotted are three categories of representative vortical structures: hairpin vortices, quasi-streamwise vortices, and interface-connected vortices. The hairpin vortex is positioned in such a way that the vorticity in the hairpin head points in the positive *y* direction. The quasi-streamwise and interface-connected vortices can rotate either way. (b) Coherent hairpin-shaped vortex structure captured with the conditional-averaging technique. Plotted is the conditionally averaged result of about 3000 instantaneous hairpin vortices.

captures the hairpin vortices and produces high-quality flow-field statistics for the quantitative study of turbulence structures. These results establish a basis for the mechanistic investigation of air-sea interaction dynamics. For example, Figure 5 shows the VISA results on a vertical cross-section of quasi-streamwise vorti-ces pointing in the -*x* direction. The contours of the streamwise vorticity component and vortex-induced velocity vectors are plotted in the left figure of Figure 5. It is shown that on the waterside, due to the induction of the vortex, the fluids to the left of the vortex are advected towards the interface and the fluids on the right are swept down. Because of this vortex-induced advection, transport of species near the interface is significantly affected. The right figure of Figure 5 shows the contours of concentration fluctuation for a passive scalar. In this study, the mean concentration value of the scalar is set initially to increase upwards. As shown

Figure 5. Conditionally averaged results of quasi-streamwise vortices based on about 3000 instantaneous events are shown. The top figure is a quasi-streamwise vortex on the water-side. Plotted are contours of streamwise vorticity component ω_x and fluctuation velocity vectors (v', w') on a vertical (y, z) cross section that is located at the center of the quasi-streamwise vortex. The waterside vortex induces a mirror vortex of the opposite sign on the air side. Between the air-water interface and the mirror vortex, there exists a micro low-level jet. The vortices and jet have a significant effect on passive scalar transport near the interface. The bottom figure shows contours of scalar concentration fluctuations.

in the figure, the vortex makes the scalar boundary layer in the left-hand-side up-welling region much thinner. As a result, transfer of the scalar across the interface is greatly enhanced there.

An important discovery from our study is the airside micro low-level jets that are induced by the water motions underneath. A typical example is shown in the VISA results of waterside upwelling motions plotted in Figure 6. As water is advected towards the interface during an upwelling, diverging flow is induced at the interface. Due to the continuity of velocity at the interface, diverging flow must also be present on the airside. Because the shear stress across the interface needs to be balanced, and because the value of dynamic viscosity of air is substantially smaller than that of water, the velocity gradient on the airside is much

larger than that on the waterside. As a result, on the airside, a jet flow in the vicinity of the interface is formed, as shown in Figure 6. Such a mechanism is also present in the case of quasi-streamwise waterside vortices. As shown in Figure 5, the negative streamwise vortex in the water induces a positive mirror vortex in the air above, as expected. What is interesting is that because of the micro low-level jet, a large vorticity of the opposite sign of the mirror vortex is formed on the airside between the induced mirror vortex and the interface. Through simulations such as these, we find that the micro low-level jet is a salient feature in air-water coupled flows and that it plays an important role in air-sea interaction dynamics.

USING FLOW STRUCTURE INFORMATION TO IMPROVE UNDERSTANDING OF FLOW STATISTICS

The knowledge of flow structures in air-sea interactions provides a basis for better understanding of flow turbulent statistics. As an example, we show the analysis of turbulent kinetic energy (TKE). TKE is defined as $k = \overline{u_i' u_i'}/2$, with u_i' the fluctuations of velocity components. TKE is an important measure of the magnitude of turbulence in atmosphere and ocean flows, and modeling the TKE budget is critical to improved understanding and prediction of coupled atmosphere-sea turbulent flows. A good understanding of the evolution of TKE and its components allows us to develop further closure models needed, for example, in larger-scale and coarser-grid simulations such as those used in mesoscale LES and Reynolds-averaged Navier-Stokes (RANS) computations. In
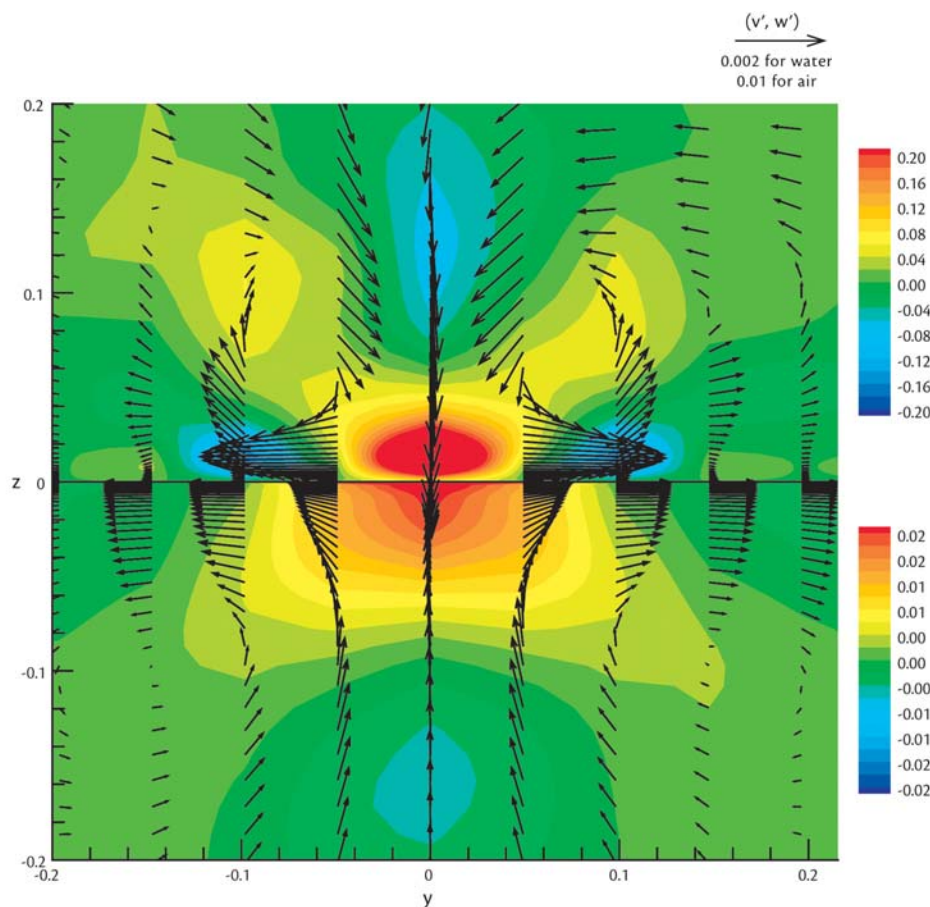

Figure 6. Conditionally averaged results of waterside upwelling based on about 3000 instantaneous events. Upwelling motion on the waterside is shown by contours of surface divergence ($\partial u/\partial x + \partial v/\partial y$) and fluctuation velocity vectors (v', w') on a vertical (y, z) cross section that is located at the center of the upwelling. Induced by the waterside upwelling, on the airside there exist a downwelling and two micro low-level jets on the edges of the downwelling. Note that in the figure, both the velocity vector scales and the contour levels of surface divergence are different between the waterside and airside.

this study, it is found that the analysis of coherent structures provides important physical insights to the mechanism of the TKE budget.

The evolution of TKE is governed by a number of processes. It is produced by the interaction between Reynolds stress and the shear in the mean flow. Meanwhile, TKE is dissipated by viscosity. In addition to these source and sink processes, TKE is transported among different flow regions by pressure fluctuations and velocity fluctuations. At regions where the TKE varies abruptly, for example, at a boundary layer, viscous diffusion also contributes to the TKE transport.

Based on the extensive data obtained from our computer simulations, we are able to perform detailed quantification and analysis of each process in the TKE budget. As shown in Figure 7, TKE production is large near the interface; viscous diffusion is only significant very close to the interface and the pressure transport is much smaller than other terms. The variation of the turbulent transport due to velocity fluctuations and the TKE dissipation is noteworthy.

Figure 7 shows that velocity fluctuations transport TKE from the bulk region of the air to the near-interface region. On the waterside, turbulence transport removes part of the TKE from the near-interface region and puts it into the deeper region. Dissipation in the air increases towards the interface and reaches a maximum at the interface, again behaving like the boundary layer near a solid wall. On the waterside, as the interface is approached, dissipation increases first, then decreases and finally increases again to reach its maximum value at the interface.

The behaviors of some of the TKE budget processes are relatively easy to understand. For example, the production term is the product of the mean shear and the Reynolds stress. As the air-water interface is approached, although the shear increases, the Reynolds stress decreases rapidly because of the constraint of vertical motions by the interface. As a result, production decreases towards the interface. The variation of the viscous diffusion and velocity transport terms is governed by the variation of velocity fluctuation profiles (Figure 3).

On the other hand, some other processes in the TKE balance are truly complex and they can only be explained based on our knowledge of the detailed vortical structures. Energy dissipation is a typical example. Our study reveals that the complicated variation of dissipation (Figure 7) is caused by the unique vortex-interaction dynamics at the air-water interface (Figures 4 and 5). On the waterside, as the interface is approached, the first peak in dissipation is associated with intense vortical activities near the interface, as evidenced by the instantaneous vortical structures plotted in Figure 4a and by the vorticity-fluctuation statistics plotted in Figure 3. Closer to the interface, horizontal vortices diminish within the surface layer. This phenomenon is similar to what we found in the free-surface turbulence case (without the air above the interface; Shen et al., 1999), where TKE dissipation is reduced and reaches a local minimum near the surface. The present case of coupled air-water flow is, however, different from the problem of free-surface turbulence in that air motions cause stress fluctuations at the interface. As a result, vorticity fluctuations and the associated TKE dissipation both reach their maxima at the interface (Figures 3 and 7). On the airside, the enhanced dissipation near the air-water interface is caused by the large shear stress at the interface and the presence of the micro low-level jets we show earlier. Such information is important for the development of turbulence modeling for the coupled air-water boundary layers.

FUTURE RESEARCH DIRECTIONS

In this study we use direct simulations to investigate the small-scale coupling dynamics of air and water turbulent flows near an air-sea interface. Through systematic high-resolution simulations, we obtain a detailed description of the velocity and vorticity fields in the coupled
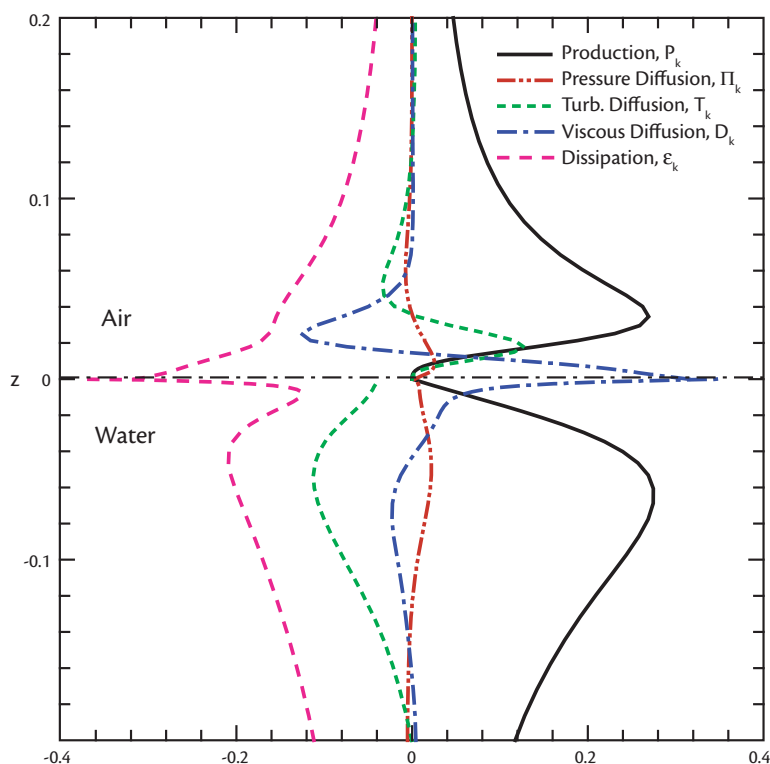
Figure 7. Processes affecting the turbulent kinetic energy (TKE) budget near the air-water interface. Shown are TKE production, dissipation, transport due to pressure fluctuation and velocity fluctuation, and viscous diffusion. All the quantities are normalized by the friction velocity at the interface and the kinematic viscosity of air and water in the corresponding regimes.

air-water turbulent flow. These data sets provide us with a physical basis to obtain high-quality flow statistics and structures. The coherent vortical structures identified in this study are found to play an important role in the near-interface transport process. Using advanced statistical tools, we are able to quantify the characteristics of those vortical structures, which in turn help us better understand and model turbulence statistics such as the TKE budget in air-sea interactions.

The physical insights obtained from this study are important for the development of turbulence modeling and prediction tools for air-sea interactions. We are now actively pursuing two fronts of research. First, we are performing a comparison with field data, in particular the data collected at the Martha's Vineyard Coastal Observatory and Air-Sea Interaction Tower during the CBLAST experiment (more information available at http://www.whoi.edu/science/AOPE/dept/CBLASTmain.html), which include wind and momentum flux profiles measured from the meteorological mask and the air-sea interaction tower (ASIT), current and wave characteristics from the ASIT, and the directional wave spectra from the offshore seanode. Our numerical simulation can be used as a powerful tool to help interpretation and syntheses of field data. For example, the TKE budget obtained from our study is valuable to the parameterization for air-ocean momentum and kinetic energy vertical transfer.

The ultimate objective is to obtain multi-scale simulation capabilities that link the finely resolved turbulent flow simulations above with truly large-scale gravity wavefield predictions. The ob-jective is to bridge the gap between the parameterization of small-scale air-sea-wave interaction physics and high-resolution regional-scale modeling of ocean waves. For the latter, our recent focus has been on developing numerical capability for the direct, phased-resolved simulation of nonlinear ocean waves for a field evolving over a distance of up to hundreds of kilometers. The key difference for these simulations is that they are based on potential-flow formulation. Computationally, potential-flow simulations can be several orders of magnitude more efficient that DNS and LES. One of the reasons for this efficiency is that potential-flow solutions generally require discretization of the boundary of the domain (which is two dimensional) versus the three-dimensional volume discretization needed for viscous/turbulent flows. In potential flow-wave simulations, viscous and turbulence effects important in phenomena such as wave-breaking dissipation and wind forcing are modeled indirectly. As it turns out, the key to success with these models lies in the types of DNS and LES turbulence simulations discussed earlier. The success of the multi-scale approach depends on our ability to integrate faithfully the effects of small-scale processes of wind-energy supply and wave-breaking dissipation on large-scale nonlinear wave evolutions. This approach builds on two advancements made recently: the numerical tools for direct phase-resolved simulation of a large-scale wave field developed at the Massachusetts Institute of Technology, and the high-performance numerical capabilities for atmosphere-ocean-wave interactions at small scales obtained at the Johns Hopkins Univer-sity (and the substantial physical understanding obtained based on simulation results). After completion, we will be capable of predicting deterministically the evolution of a large-scale ($O(10^{3\sim4}km^2)$) nonlinear ocean wave-field in realistic marine environments with the presence of high winds and whitecapping.

REFERENCES

Adrian, R.J., and P. Moin. 1988. Stochastic estimation of organized turbulent structure—Homogeneous shear flow. *Journal of Fluid Mechanics* 190:531–559.

Blackwelder, R.F., and R.E. Kaplan. 1976. On the wall structure of the turbulent boundary layer. *Journal of Fluid Mechanics* 76:89–112.

Jeong, J., and F. Hussain. 1995. On the identification of a vortex. *Journal of Fluid Mechanics* 482:319–345.

Kim, J. 1983. On the structure of wall-bounded turbulent flows. *Physics of Fluids* 26:2,088–2,097.

Liu, S. 2005. *Numerical Investigation of Turbulent Coupling Boundary Layer of Air-Water Interaction Flow*. Master's thesis. Massachusetts Institute of Technology, Cambridge, MA.

Moin, P., and K. Mahesh. 1998. Direct numerical simulation: A tool in turbulence research. *Annual Reviews of Fluid Mechanics* 30:539–578.

Robinson, S.K. 1991. Coherent motions in the turbulent boundary layer. *Annual Reviews of Fluid Mechanics* 23:601–639.

Shen, L., and D.K.P. Yue. 2001. Large-eddy simulation of free-surface turbulence. *Journal of Fluid Mechanics* 440:75–116.

Shen, L., X. Zhang, D.K.P. Yue, and G.S. Triantafyllou. 1999. The surface layer for free-surface turbulent flows. *Journal of Fluid Mechanics* 386:167–212.